

# Uptake of H<sub>2</sub><sup>17</sup>O(g) and D<sub>2</sub>O(g) by Aqueous Sulfuric Acid Droplets

Michael Gershenson<sup>†</sup> and Paul Davidovits

Department of Chemistry, Boston College, Chestnut Hill, Massachusetts 02467-3809

Leah R. Williams,\* Quan Shi, John T. Jayne, Charles E. Kolb, and Douglas R. Worsnop

Center for Aerosol and Cloud Chemistry, Aerodyne Research, Inc., Billerica, Massachusetts 01821-3976

Received: August 12, 2003; In Final Form: December 20, 2003

We report here the first experimental determination of the mass accommodation coefficient ( $\alpha$ ) of H<sub>2</sub><sup>17</sup>O(g) on aqueous sulfuric acid solutions. The uptake of <sup>17</sup>O-labeled gas-phase water was measured as a function of temperature (250–295 K) and acid concentration (50–82 wt % H<sub>2</sub>SO<sub>4</sub>) using a droplet train flow reactor. The mass accommodation coefficient exhibits a negative temperature dependence and increases with increasing H<sub>2</sub>SO<sub>4</sub> concentration. For 50 wt % sulfuric acid solution, the mass accommodation coefficient ranges from  $0.50 \pm 0.05$  at 250 K to  $0.41 \pm 0.07$  at 278 K, and for 70 wt % solution, it ranges from  $0.69 \pm 0.07$  at 252 K to  $0.54 \pm 0.05$  at 295 K. The dependence of the mass accommodation coefficient on the sulfuric acid composition correlates with surface coverage of water. The uptake coefficient of D<sub>2</sub>O was measured to be unity on 70 wt % H<sub>2</sub>SO<sub>4</sub>, independent of temperature between 263 and 293 K. The D<sub>2</sub>O uptake coefficient is larger than the mass accommodation coefficient for H<sub>2</sub><sup>17</sup>O because D–H isotope exchange opens another channel for the disappearance of D<sub>2</sub>O from the gas phase. The D<sub>2</sub>O uptake coefficient of unity implies that the thermal accommodation coefficient of water on sulfuric acid surfaces is also unity.

## Introduction

The amount of solar energy scattered, reflected, or absorbed by clouds is determined by “cloud optical properties,” a term that encompasses size and number distributions of cloud droplets as well as chemical composition. The ability to predict both short-term meteorology and long-term climate change rests on detailed understanding of the dynamic processes governing aerosol activation and growth to form cloud droplets. By far the largest uncertainty in quantifying the driving forces of anthropogenic climate change is attributed to man-made sub-micron aerosol particles capable of cloud nucleation.<sup>1</sup>

The now classic Köhler theory of cloud droplet formation and growth relies on the assumption that the particle size is always in equilibrium with the local supersaturation of water vapor.<sup>2</sup> According to Köhler’s equation, cloud droplets grow spontaneously after they have reached a critical diameter,  $D_c$ , which corresponds to a critical supersaturation,  $S_c$ . Hence, the highest supersaturation attained in an ascending air parcel defines the total number of activated aerosol particles that will grow to cloud droplets. However, this equilibrium relationship is not always valid.<sup>3–5</sup> For example, if the mass transfer of gaseous water into pre-existing aqueous aerosol particles is kinetically hindered, a higher supersaturation will build up in an air parcel, activating a greater fraction of available aerosol seeds.

The parameter representing the interfacial rate for gas–liquid mass transfer is usually designated as the mass accommodation coefficient,  $\alpha$ , i.e., the probability that a molecule impinging on a liquid surface penetrates that surface and becomes incorporated into the bulk liquid. In a previous paper,<sup>6</sup> we

reported the mass accommodation coefficients for water on water. This work on the mass accommodation coefficient of water on sulfuric acid builds on the measurements of Li et al.<sup>6</sup> In the work of Li et al.,<sup>6</sup> the mass accommodation coefficient of water vapor on water was determined by measuring the uptake of <sup>17</sup>O-labeled gas-phase water under near-equilibrium conditions. The values of  $\alpha$  for water vapor on water were found to range from  $0.17 \pm 0.03$  to  $0.32 \pm 0.04$  between 280 and 258 K.

In the work presented here, we report the first measurements of the mass accommodation coefficient of water vapor on sulfuric acid droplets as a function of temperature ( $T = 250$ – $295$  K) and sulfuric acid concentration (50–82 wt %). The values of the mass accommodation coefficient are in the range of  $\sim 0.4$  to unity depending on acid concentration and temperature. In addition, the uptake of D<sub>2</sub>O by 70 wt % H<sub>2</sub>SO<sub>4</sub> solution was measured to be unity within experimental error at 263 and 293 K. From the results of the D<sub>2</sub>O uptake measurements, and following the analysis presented in Li et al.,<sup>6</sup> we conclude that the thermal accommodation coefficient of water on 50 to 80 wt % sulfuric acid solutions is unity.

**Uptake of Gases by Liquids.** The mass accommodation coefficient,  $\alpha$ , governs the maximum possible flux,  $J$  (molecule m<sup>-2</sup> s<sup>-1</sup>), of gas molecules into a liquid in the absence of surface reactions

$$J = \frac{n_g \bar{c} \alpha}{4} \quad (1)$$

Here  $n_g \bar{c}/4$  is the gas–surface collision rate from gas-kinetic theory where  $n_g$  (molecule m<sup>-3</sup>) is the gas molecular density and  $\bar{c}$  (m s<sup>-1</sup>) is the average thermal velocity. If reactions occur at the gas–liquid interface, for example, isotope exchange, then

\* Author to whom correspondence may be addressed. E-mail: Williams@aerodyne.com.

<sup>†</sup> Current address: Sandia National Laboratories, Livermore, CA 94551.

the flux of molecules disappearing from the gas phase can exceed that determined by  $\alpha$ .

The flux of gas-phase molecules into a liquid can be controlled by several other processes in addition to  $\alpha$  and surface reactions: gas-phase diffusion, Henry's law saturation, and liquid bulk-phase reactions. In the case of water uptake by sulfuric acid droplets, gas-phase diffusion and Henry's law saturation are important, but no liquid-phase reactions are expected. The flux limitation due to gas-phase diffusion arises if the diffusion rate of the trace species is not fast enough to counteract the concentration gradient near the surface created by uptake by the liquid. Henry's law saturation refers to the fact that some fraction of the molecules that enter the liquid can evaporate back into the gas phase due to the limited solubility of the species. As the exposure time increases, the liquid-phase concentration reaches saturation and the evaporating flux increases, thus decreasing the net flux into the liquid. The net flux of molecules given these limitations is described by a measured uptake coefficient,  $\gamma_{\text{meas}}$

$$J_{\text{meas}} = \frac{n_g \bar{c} \gamma_{\text{meas}}}{4} \quad (2)$$

Since  $\gamma_{\text{meas}}$  represents a convolution of several processes, the experimental challenge is to separate the contributions of these processes to the overall gas uptake. The droplet train flow reactor allows direct control of many of the factors contributing to gas uptake and thereby enables deconvolution of the uptake into its component processes.<sup>7–10</sup>

The time, temperature, pressure, and concentration dependences of the measured uptake coefficient,  $\gamma_{\text{meas}}$ , can be analyzed to yield information about the chemical and physical processes occurring during the gas/liquid interaction. These processes are coupled, and general solutions for the coupled differential equations describing the gas/liquid interaction are not available, although exact solutions exist for a few limited cases.<sup>11</sup> However, to a very good approximation, the processes can be decoupled and treated separately with linear approximations to the differential equations.<sup>8,12</sup>  $\gamma_{\text{meas}}$  is then described in terms of dimensionless conductances,  $\Gamma_{\text{diff}}$ ,  $\alpha$ , and  $\Gamma_{\text{sat}}$ ,<sup>13</sup> representing gas-phase diffusion, mass accommodation, and Henry's law saturation, respectively, as follows

$$\frac{1}{\gamma_{\text{meas}}} = \frac{1}{\Gamma_{\text{diff}}} + \frac{1}{\alpha} = \frac{1}{\Gamma_{\text{sat}}} \quad (3)$$

Analytical equations for gas-phase diffusive transport of a trace gas to a train of moving droplets do not exist. However, an empirical formulation of diffusive transport to a stationary droplet developed by Fuchs and Sutugin<sup>14</sup> has been shown to be in good agreement with measurements<sup>15,16</sup> and can be modified for use with a train of moving droplets. By use of the Fuchs–Sutugin formulation,  $\Gamma_{\text{diff}}$  for a single droplet is expressed as<sup>17</sup>

$$\frac{1}{\Gamma_{\text{diff}}} = \frac{0.75 + 0.283Kn}{Kn(1 + Kn)} \quad (4)$$

where the Knudsen number,  $Kn = 2\lambda/d_f$ ,  $\lambda$  (m) =  $3D_g/\bar{c}$ , is the gas-phase mean free path,  $d_f$  (m) is the droplet diameter, and  $D_g$  (m<sup>2</sup> s<sup>-1</sup>) is the gas-phase diffusion coefficient. In a train of moving droplets, the Fuchs–Sutugin expression is modified by setting

$$Kn = \lambda/d_0 \quad (5)$$

where  $d_0$  (m) is the diameter of the droplet-forming orifice. Note that the effective Knudsen number defined by eq 5 for calculating the gas-phase diffusion correction in the droplet train experiments depends on the orifice diameter and not on the diameter of the droplets. Expression 5 for the effective Knudsen number was determined empirically from droplet train flow reactor experiments over a wide range of Knudsen numbers, gas mixtures, and uptake coefficients.<sup>18</sup> Recent theoretical calculations of gas-phase diffusion in a droplet train flow reactor by Morita et al.<sup>19</sup> support the conclusion that the effective Knudsen number depends on the orifice diameter rather than the droplet diameter.

The expression for  $\Gamma_{\text{sat}}$  in the droplet train apparatus is

$$\frac{1}{\Gamma_{\text{sat}}} = \frac{\bar{c}}{8RTH} \left( \frac{\pi t}{D_l} \right)^{1/2} \quad (6)$$

where  $R$  (L atm mol<sup>-1</sup> K<sup>-1</sup>) is the gas constant,  $T$  (K) is the gas-phase temperature,  $H$  (M atm<sup>-1</sup>) is the Henry's law constant,  $D_l$  (m<sup>2</sup> s<sup>-1</sup>) is the liquid-phase diffusion coefficient of the trace species, and  $t$  (s) is the gas–liquid interaction time. Note that  $1/\Gamma_{\text{sat}}$  is time-dependent so that the effect of Henry's law saturation is a decrease with time of the overall uptake coefficient,  $\gamma_{\text{meas}}$ .

Mass accommodation can be viewed as a two-step process involving surface adsorption followed by a competition between desorption and solvation.<sup>10,20</sup> First, the gas molecule strikes the surface and is thermally accommodated. The adsorption rate constant is  $k_{\text{ads}} = S\bar{c}/4$ , where  $S$  is the thermal accommodation coefficient, defined as the probability that a water vapor molecule striking the liquid will thermally equilibrate with the surface. The adsorbed surface species then either enters the liquid ( $k_{\text{sol}}$ ) or desorbs ( $k_{\text{des}}$ ) from the surface. Evaporation of the species out of the bulk liquid is taken into account separately, via the term  $\Gamma_{\text{sat}}$  in eq 3. Solving the rate equations for the mass accommodation process leads to<sup>10</sup>

$$\frac{\alpha}{S - \alpha} = \frac{k_{\text{sol}}}{k_{\text{des}}} \quad (7)$$

Note that definitions of  $\alpha$  and  $S$  differ from those used in analogous discussions of gas sticking on ice surfaces.<sup>21</sup> Specifically, the definition of  $\alpha$  given in Brown et al.<sup>21</sup> takes into account the flux of gas molecules desorbing from the surface; their definition of  $S$  is referenced to the incoming flux of gas molecules rather than to the maximum theoretical rate of gas–surface collisions predicted by gas kinetic theory.

In the D<sub>2</sub>O uptake experiments, D–H isotope exchange at the surface opens a new channel for the disappearance of the gas-phase species. In the presence of a surface reaction, such as isotope exchange, the expression for  $\gamma_0$ , i.e., the uptake coefficient corrected for gas-phase diffusion, is given by<sup>22</sup>

$$\frac{1}{\gamma_0} = \frac{1}{\gamma_{\text{meas}}} - \frac{1}{\Gamma_{\text{diff}}} = \frac{1}{S} + \frac{1}{\frac{1}{\Gamma_b} + \frac{1}{S \frac{k_{\text{sol}}}{k_{\text{des}}} + \Gamma_s}} \quad (8)$$

Here  $\Gamma_s$  corresponds to reactive loss of D<sub>2</sub>O at the surface due to isotope exchange and  $\Gamma_b$  corresponds to reactive loss in the bulk of any D<sub>2</sub>O that gets incorporated into the liquid.

## Experimental Technique

A schematic of the droplet train flow reactor is shown in Figure 1 (see Worsnop et al.<sup>7</sup> and Robinson et al.<sup>23</sup> for details).

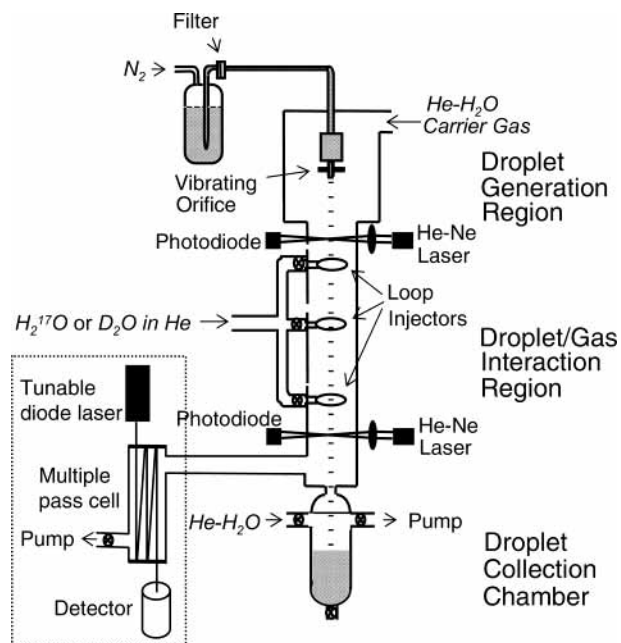


**Figure 1.** Schematic of the droplet train flow reactor apparatus.

Gas-uptake coefficients are measured by passing a fast-moving ( $30 \text{ m s}^{-1}$ ), monodisperse ( $\sim 2 \times 10^{-4} \text{ m}$  diameter) collimated train of liquid droplets through a  $0.33\text{-m}$  long,  $1.7 \times 10^{-2}\text{-m}$  diameter longitudinal low-pressure  $533\text{--}1066\text{-Pa}$  ( $4\text{--}8$  Torr) flow tube. The trace gas of interest, in this case,  $\text{H}_2^{17}\text{O}$  or  $\text{D}_2\text{O}$ , is introduced through one of three loop injectors located along the flow tube at a density of  $10^{19}\text{--}10^{20} \text{ molecule m}^{-3}$ . By selecting the gas inlet port and the speed of the droplets, the gas–droplet interaction time can be varied between  $2$  and  $15 \times 10^{-3} \text{ s}$ .

The droplet stream is produced by forcing the sulfuric acid/water solutions through a  $70\text{-}\mu\text{m}$  diameter platinum electron microscope aperture surrounded by a donut-shaped piezoelectric ceramic. For a given liquid flow rate (typically  $10^{-7} \text{ m}^3 \text{ s}^{-1}$ ), the number of droplets produced per second and their diameter is determined by the driving frequency applied to the piezoelectric ceramic. The driving frequency was switched between around  $10 \text{ kHz}$  and around  $50 \text{ kHz}$ , generating droplets with diameters of  $2.8 \times 10^{-4}$  and  $1.6 \times 10^{-4} \text{ m}$ , respectively. The sulfuric acid was cooled to the desired temperature before entering the vibrating orifice.

The droplet velocity ( $\sim 30 \text{ m s}^{-1}$ ), shape, and uniformity were monitored by measuring the light intensity from two cylindrically focused He–Ne laser beams passing through different heights along the droplet stream. Each time a droplet interrupts the light beam, the decrease in intensity is measured by a photodiode. The relative intensity of the signal reflects the relative droplet diameter. The measured time delay between the signals detected by two diodes separated by a known distance is converted to droplet velocity. Furthermore, a time trace of the HeNe signal provides a measurement of the quality of droplets. It has been shown that for a single well-defined spherical droplet, the signal shape is Gaussian; significant deviations from a Gaussian indicate low quality of the droplets (for details see Worsnop et al.<sup>7</sup>).

Carrier gas enters the flow tube at the top, giving a total flow tube pressure of  $533\text{--}1066 \text{ Pa}$  ( $4\text{--}8$  Torr). The carrier gas is a mixture of helium and water vapor, with the water vapor concentration set to match the equilibrium water vapor of the sulfuric acid at the temperature of the droplets. The precise match of the water vapor pressure in contact with the droplets

ensures that no evaporation or condensation of water occurs and that the temperature and composition of the droplets are stable. Typical volume flow rates of the carrier gas were  $4\text{--}7 \times 10^{-6} \text{ m}^3 \text{ s}^{-1}$  at standard temperature and pressure, giving a linear gas velocity of  $2.6\text{--}4.4 \text{ m s}^{-1}$ .

Uptake coefficients are measured by switching the droplet-generating frequency and thus the surface area of the droplets. A measured decrease in the trace gas concentration resulting from an increase in the exposed droplet surface area corresponds to uptake of the gas by the droplet surface. The number density of the trace gas,  $n_g$  ( $\text{molecule m}^{-3}$ ), is measured downstream of the flow tube by infrared absorption using a lead–salt tunable diode laser coupled to a multipass absorption cell.<sup>24</sup>  $\text{H}_2^{17}\text{O}$  was monitored at  $1632.1667 \text{ cm}^{-1}$  and  $\text{D}_2\text{O}$  at  $1239.0457 \text{ cm}^{-1}$ .<sup>25,26</sup> The measured uptake coefficient is obtained from the experimental parameters as shown in eq 9<sup>7</sup>

$$\gamma_{\text{meas}} = \frac{4F_g}{c\Delta A} \ln \frac{n_g}{n'_g} \quad (9)$$

where  $F_g$  ( $\text{m}^3 \text{ s}^{-1}$ ) is the carrier gas volume rate of flow through the system,  $\Delta A$  ( $\text{m}^2$ ) is the change in the total droplet surface area in contact with the trace gas when the driving frequency is switched, and  $n_g$  and  $n'_g$  are the trace gas densities at the two surface areas. Typical differences between  $n_g$  and  $n'_g$  are in the range of  $10\text{--}30\%$ .

Measurements of the mass accommodation coefficient for  $\text{H}_2\text{O}(\text{g})$  were made by determining the uptake of the isotope  $\text{H}_2^{17}\text{O}(\text{g})$  on  $50$ ,  $70$ , and  $82 \text{ wt } \%$  sulfuric acid droplets over the temperature range  $250\text{--}295 \text{ K}$ . Interactions between  $\text{H}_2\text{O}(\text{g})$  and the sulfuric acid/water liquid surface are likely to depend on hydrogen bonding, and thus the mass accommodation coefficient is not expected to change due to isotope substitution of the oxygen. The natural abundance of  $^{17}\text{O}$  is  $3.7 \times 10^{-4}$ , and there is therefore a background of  $\text{H}_2^{17}\text{O}(\text{g})$  in the flow tube from the water vapor in equilibrium with the droplets. Depending on the temperature and composition of the droplets, the  $\text{H}_2^{17}\text{O}(\text{g})$  background is on the order of  $2\text{--}5 \times 10^{18} \text{ molecule m}^{-3}$ . Additional  $\text{H}_2^{17}\text{O}(\text{g})$  on the order of  $10^{19}\text{--}10^{20} \text{ molecule m}^{-3}$  is introduced into the flow tube by flowing He through a bubbler containing  $20\%$   $\text{H}_2^{17}\text{O}$  in  $\text{H}_2\text{O}$ . The  $\text{H}_2\text{O}$  entrained in the He causes a  $0.3\text{--}10\%$  increase in the background water vapor in the flow tube. The perturbation of the water vapor concentration in the flow tube leads to an increase of the droplet temperature by  $0.1\text{--}3 \text{ K}$  due to the release of the heat of condensation as the droplet reaches equilibrium with the surrounding water vapor. The background concentration of  $\text{H}_2^{17}\text{O}(\text{g})$  was monitored and was taken into account in calculating  $\gamma_{\text{meas}}$ . In the experiments with  $\text{D}_2\text{O}$ , the natural abundance of  $\text{D}$  is on the order of  $10^{-7}$  and can be neglected.

A small amount of  $\text{CH}_4$  is introduced with the trace gas and used as an inert tracer to monitor changes in pressure in the flow tube. The  $\text{CH}_4$  concentration is monitored by infrared absorption at the  $1632.1093$  and  $1632.1167 \text{ cm}^{-1}$  doublet<sup>25</sup> simultaneously with the trace species. Methane is expected to be insoluble in sulfuric acid, and any changes in concentration upon switching the droplet frequency reflect changes in flow tube pressure. The measured uptake coefficient was corrected for the observed  $\text{CH}_4$  changes. The correction due to pressure variation was usually around  $3\%$  and always less than  $10\%$ .

Loss of the gas-phase trace species to the flow tube walls was small in these experiments. In the  $\text{D}_2\text{O}$  experiments, we measured the wall loss by turning off the droplets and testing for any change in the  $\text{D}_2\text{O}$  concentration when changing loop



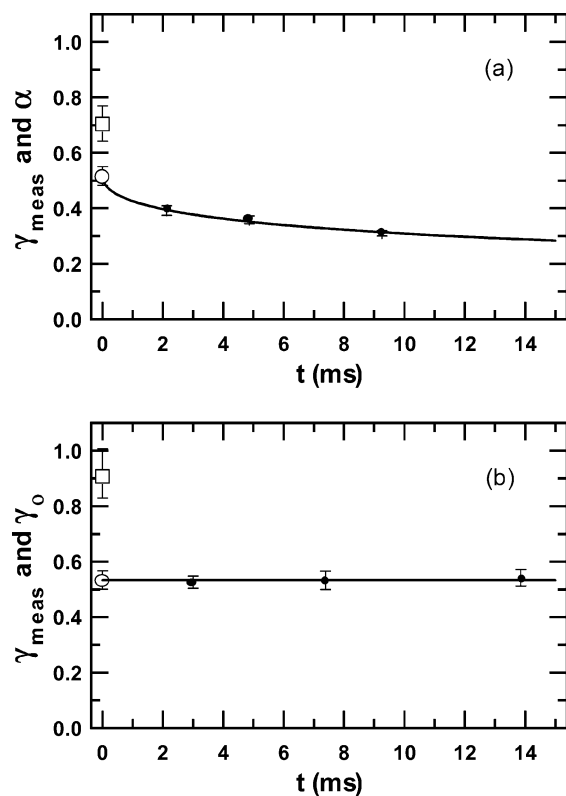


**Figure 2.** (a) Measured uptake coefficient,  $\gamma_{\text{meas}}$ , for  $\text{H}_2^{17}\text{O}(\text{g})$  on 70 wt % sulfuric acid at 263 K (●) and fit to the data with eq 3 (solid line). Extrapolation of the time dependence (eq 6) back to  $t = 0$  gives the ○, and correction for gas-phase diffusion (eq 4) gives  $\alpha = 0.70 + 0.07/-0.06$  (□). (b) Measured uptake coefficient for  $\text{D}_2\text{O}(\text{g})$  on 70 wt % sulfuric acid at 263 K (●). Correction for gas-phase diffusion gives  $\gamma_0 = 0.91 + 0.1/-0.08$  (□).

injectors. No change was observed. The uncertainty in the  $\text{D}_2\text{O}$  concentration measurement ( $<1\%$ ) gives an upper limit for the wall loss of  $k_w < 0.06 \text{ m}^{-1}$ , where the wall-loss coefficient is defined as  $n(z)/n(0) = \exp(-k_w z)$ . In terms of the gas-wall interaction time, the wall-loss coefficient is  $k_{w-t} < 0.3 \text{ s}^{-1}$  where  $k_w$  and  $k_{w-t}$  are related by the gas-flow velocity,  $k_{w-t} = k_w v_f$  ( $v_f = 4.9 \text{ m s}^{-1}$  in this case). The value of  $k_w < 0.06 \text{ m}^{-1}$  corresponds to a wall uptake coefficient of  $\gamma_w < 10^{-5}$ , 2 orders of magnitude smaller than the smallest  $\gamma$  measurable with the droplet train flow reactor. In the  $\text{H}_2^{17}\text{O}$  experiments, wall loss was also below our detection limit.

## Results and Analysis

Figure 2a shows the measured uptake coefficient for  $\text{H}_2^{17}\text{O}(\text{g})$  on 70 wt % sulfuric acid at 263 K as a function of gas-droplet contact time.  $\gamma_{\text{meas}}$  was calculated (using eq 9) from the observed change in trace gas density upon switching the droplet generation frequency. Multiple measurements (5–7) were made at each contact time, and the error bars show the  $1\sigma$  scatter in the data. The overall experimental uncertainty in  $\gamma_{\text{meas}}$  is  $\pm 8\%$  based on the scatter in the data. This is consistent with the estimated experimental uncertainty ( $\pm 7\%$ ) obtained by propagating the errors in each of the measured quantities in eq 9.

The data in Figure 2a show that the measured uptake coefficient decreases by about 25% during the 10-ms gas-liquid contact time. Time-dependent uptake coefficients suggest that the uptake process is affected by the solubility constraints (via  $\Gamma_{\text{sat}}$ ) of the trace species in the liquid. The solid line in Figure 2a shows the fit to the data using eqs 3 and 6. The fit yields a value for  $H_{\text{meas}}D_1^{1/2}$  of  $(4.3 \pm 0.6) \times 10^{-1} \text{ M m atm}^{-1} \text{ s}^{-1/2}$ .

The coefficient  $H_{\text{meas}}$  can be calculated from the product  $H_{\text{meas}}D_1^{1/2}$  using an estimated  $D_1$  for water in sulfuric acid. The liquid-phase diffusion coefficient is estimated from the equation

$$D_1 = cT/\eta \quad (10)$$

where  $\eta$  (cp) is the liquid viscosity and  $c$  is a constant calculated to be  $c = 6.5 \times 10^{-12} \text{ m}^2 \text{ cp s}^{-1} \text{ K}^{-1}$  from the experimental data on water viscosity and water self-diffusion.<sup>27</sup> For the conditions of the data in Figure 2a, the viscosity of the sulfuric acid is 29.8 cp<sup>28</sup> and the estimated liquid-phase diffusion  $D_1$  is  $5.7 \times 10^{-11} \text{ m}^2 \text{ s}^{-1}$ , yielding  $H_{\text{meas}} = 5.7 \times 10^4 \text{ M atm}^{-1}$ .

When eq 6 is applied to trace gas uptake, the parameter  $H$  is the Henry's law coefficient defined in the limit of the solute concentration approaching zero. However,  $\text{H}_2^{17}\text{O}(\text{g})$  enters sulfuric acid solutions that contain water at high concentrations (18–40 M). In this case, the  $H$  value extracted from eq 6 cannot be considered as a true Henry's law coefficient.  $H$  obtained here is simply a fitting parameter.<sup>29</sup>

Fitting the time-dependent data in Figure 2a with eq 6 gives a value for  $\gamma$  at  $t = 0$  shown with the open circle. The error bars are the statistical uncertainty from the fit ( $\pm 8\%$ ). The correction for gas-phase diffusion is applied using eq 4 to calculate  $1/\Gamma_{\text{diff}}$ .  $D_g$  for  $\text{H}_2\text{O}$  in He is  $8.4 \times 10^{-5} \text{ atm m}^2 \text{ s}^{-1}$  at 293 K,<sup>30</sup> and  $D_g$  for  $\text{H}_2\text{O}$  in  $\text{H}_2\text{O}$  is  $1.5 \times 10^{-5} \text{ atm m}^2 \text{ s}^{-1}$  at 293 K,<sup>31</sup> both with a temperature dependence of  $T^{1.5}$ .  $D_g$  for  $\text{D}_2\text{O}$  is a few percent smaller than the corresponding  $D_g$  for  $\text{H}_2\text{O}$ ,<sup>32</sup> and this difference was neglected. Values of the effective  $D_g$  for the conditions in the flow tube were calculated using the standard formula for mixtures of gases.<sup>33</sup>

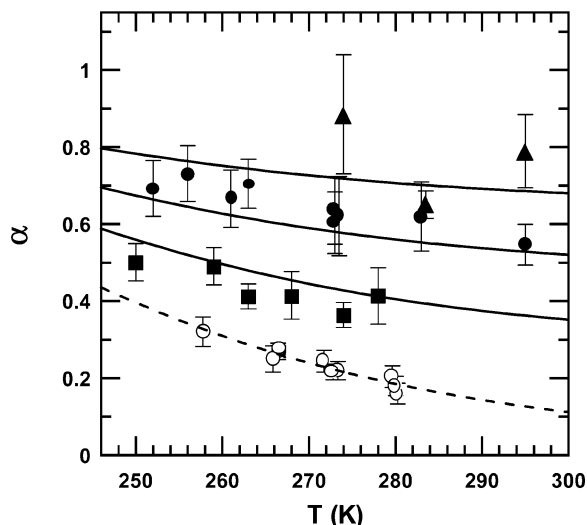
The value for  $\alpha$  obtained by correcting  $\gamma$  at  $t = 0$  for the effect of gas-phase diffusion is  $0.70 + 0.07/-0.06$  and is shown with the open square in Figure 2a. The error bars include a  $\pm 5\%$  uncertainty in  $D_g$  as well as the uncertainty in  $\gamma$  at  $t = 0$  and are slightly asymmetric because the gas-phase diffusion correction is nonlinear.

Figure 2b shows the uptake data for  $\text{D}_2\text{O}$  on 70 wt % sulfuric acid droplets at 263 K. The data exhibit no time dependence, and the open circle at  $t = 0$  is the average of the three data points. After correcting for gas-phase diffusion,  $\gamma_0 = 0.91 + 0.09/-0.08$  for this particular data set. Note that the gas-phase diffusion correction was larger for the  $\text{D}_2\text{O}$  data in Figure 2b than for the  $\text{H}_2^{17}\text{O}$  data in Figure 2a because the total flow tube pressure was higher. Averaging over three different experimental runs gave  $\gamma_0 = 0.93 + 0.11/-0.10$ . No temperature dependence was observed for the uptake coefficient of  $\text{D}_2\text{O}$  on 70 wt % sulfuric acid droplets between 263 and 293 K.

The mass accommodation coefficient for  $\text{H}_2^{17}\text{O}(\text{g})$  on sulfuric acid solutions was measured as a function of temperature for three different sulfuric acid concentrations, 50, 70, and 82 wt %. The results are shown in Figure 3, along with previous data for the mass accommodation of  $\text{H}_2^{17}\text{O}(\text{g})$  on water.<sup>6</sup> (Note that the 82 wt % data points have large error bars due to the difficulty of forming droplets with such a viscous solution.) The mass accommodation coefficient decreases as the temperature increases. A negative temperature dependence for  $\alpha$  has been previously observed for a wide variety of hydrophilic gas-phase species interacting with aqueous surfaces.<sup>34,35</sup> The temperature dependence can be expressed as

$$\frac{\alpha}{1-\alpha} = \exp\left(\frac{-\Delta G_{\text{obs}}}{RT}\right) = \left[\exp\left(\frac{\Delta S_{\text{obs}}}{R}\right)\right] \exp\left(\frac{-\Delta H_{\text{obs}}}{RT}\right) \quad (11)$$

where  $\Delta G_{\text{obs}} = \Delta H_{\text{obs}} - T\Delta S_{\text{obs}}$  is the Gibbs energy of the transition state between the gas-phase and the aqueous solvated



**Figure 3.** Mass accommodation coefficient,  $\alpha$ , for H<sub>2</sub><sup>17</sup>O(g) on 82 (▲), 70 (●), and 50 wt % (■) sulfuric acid solutions and on water (○)<sup>6</sup> as a function of temperature. The solid lines are from eq 12, and the dashed line is a fit to the water data with eq 11.

phase. The dashed line drawn through the water data points (open circles) in Figure 3 is the fit to eq 11, yielding  $\Delta H_{\text{obs}} = 4.8 \pm 0.5$  kcal/mol and  $\Delta S_{\text{obs}} = 20.3 \pm 1.8$  cal/mol K.

As can be seen in Figure 3, the mass accommodation coefficient of H<sub>2</sub><sup>17</sup>O(g) on sulfuric acid–water mixtures increases with increasing sulfuric acid concentration. We modeled this increase as a linear combination of mass accommodation coefficients on a two component liquid system<sup>36</sup>

$$\alpha = \alpha_{\text{H}_2\text{O}}X(s)_{\text{H}_2\text{O}} + \alpha_{\text{H}_2\text{SO}_4}X(s)_{\text{H}_2\text{SO}_4} = \alpha_{\text{H}_2\text{O}}X(s)_{\text{H}_2\text{O}} + \alpha_{\text{H}_2\text{SO}_4}(1 - X(s)_{\text{H}_2\text{O}}) \quad (12)$$

where  $\alpha_{\text{H}_2\text{O}}$  is the mass accommodation coefficient for H<sub>2</sub><sup>17</sup>O(g) on water,  $\alpha_{\text{H}_2\text{SO}_4}$  is the mass accommodation coefficient for H<sub>2</sub><sup>17</sup>O(g) on sulfuric acid,  $X(s)_{\text{H}_2\text{O}}$  is the fractional surface coverage of water, and  $X(s)_{\text{H}_2\text{SO}_4}$  is the fractional surface coverage of H<sub>2</sub>SO<sub>4</sub>. The fractional surface coverage of water was calculated from the following two equations

$$\Gamma_{\text{H}_2\text{O}} = N_{\text{H}_2\text{O}}^s - N_{\text{H}_2\text{SO}_4}^s X_{\text{H}_2\text{O}}/X_{\text{H}_2\text{SO}_4} \quad (13)$$

where  $\Gamma_{\text{H}_2\text{O}}$  is the Gibbs surface excess of H<sub>2</sub>O,  $N_{\text{H}_2\text{O}}^s$  and  $N_{\text{H}_2\text{SO}_4}^s$  are the surface concentrations of H<sub>2</sub>O and H<sub>2</sub>SO<sub>4</sub> (molecule m<sup>-2</sup>) and  $X_{\text{H}_2\text{O}}$  and  $X_{\text{H}_2\text{SO}_4}$  are the bulk phase mole fractions, and

$$A_{\text{H}_2\text{O}}N_{\text{H}_2\text{O}}^s + A_{\text{H}_2\text{SO}_4}N_{\text{H}_2\text{SO}_4}^s = 1 \quad (14)$$

where  $A_{\text{H}_2\text{O}}$  and  $A_{\text{H}_2\text{SO}_4}$  (m<sup>2</sup>) are the molecular areas, and  $A_{\text{H}_2\text{O}}N_{\text{H}_2\text{O}}^s$  is the fractional surface coverage,  $X(s)_{\text{H}_2\text{O}}$ . Phillips calculated values for  $\Gamma_{\text{H}_2\text{O}}$  from surface tension data.<sup>37</sup> Values for  $A_{\text{H}_2\text{O}} = 0.97 \times 10^{-19}$  m<sup>2</sup> and  $A_{\text{H}_2\text{SO}_4} = 1.9 \times 10^{-19}$  m<sup>2</sup> were calculated from data in Phillips.<sup>37</sup>

The solid lines in Figure 3 show eq 12 plotted for the sulfuric acid concentrations used in our experiments. We have assumed  $\alpha_{\text{H}_2\text{SO}_4} = 1$ , based on the increase of  $\alpha$  toward unity with increasing sulfuric acid concentration. Table 1 gives values for the calculated  $N_{\text{H}_2\text{O}}^s$  and  $X(s)_{\text{H}_2\text{O}}$ , the experimentally measured  $\alpha$ , and the  $\alpha$  calculated from eq 12. The agreement between the measured and modeled values of  $\alpha$  is quite good.

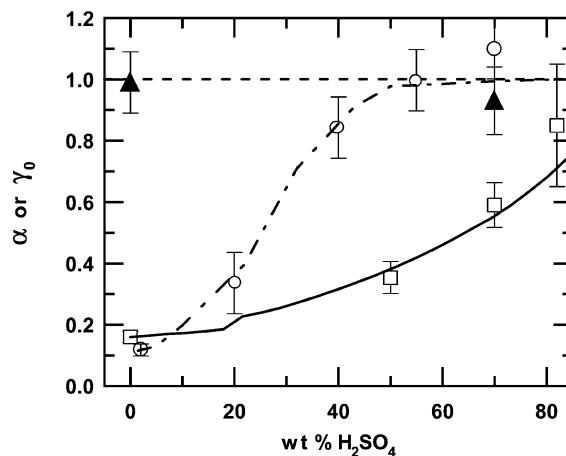


**Figure 4.** A plot of interfacial uptake coefficients ( $\alpha$  or  $\gamma_0$ ) as a function of sulfuric acid concentration for H<sub>2</sub><sup>17</sup>O(g) (□), D<sub>2</sub>O(g) (▲), and NH<sub>3</sub>(g) (○) at 285K. The dash–dot line is the surface reaction model for NH<sub>3</sub>(g) uptake. The solid line is eq 12 for the mass accommodation of H<sub>2</sub><sup>17</sup>O(g), and the dashed line is a guide for the eye at unity.

**TABLE 1: Calculated Surface Density of H<sub>2</sub>O at 298 K,  $N_{\text{H}_2\text{O}}^s$ , Calculated Fractional Surface Coverage of H<sub>2</sub>O,  $X(s)_{\text{H}_2\text{O}}$ , Measured  $\alpha$  at 285 K, and the Value of  $\alpha$  Calculated from eq 12**

wt % H <sub>2</sub> SO <sub>4</sub>	$N_{\text{H}_2\text{O}}^s$ , m <sup>-2</sup>	$X(s)_{\text{H}_2\text{O}}$	$\alpha$ , 285 K	$\alpha$ , eq 12
0	$1.05 \times 10^{19}$	1	$0.16 \pm 0.02$	0.16
50	$7.7 \times 10^{18}$	0.73	$0.35 \pm 0.05$	0.38
70	$5.5 \times 10^{18}$	0.52	$0.59 \pm 0.07$	0.55
82	$3.4 \times 10^{18}$	0.32	$0.85 \pm 0.2$	0.71

The nature of aqueous sulfuric acid surfaces has been the subject of recent spectroscopic studies. Sum frequency generation, a surface specific technique, indicates that the amount of free water at the surface decreases with increasing sulfuric acid concentration.<sup>38</sup> A decrease in free water is consistent with calculations of molecular hydrate (i.e., H<sub>2</sub>SO<sub>4</sub>·*n*H<sub>2</sub>O with *n* = 1, 2) formation at the sulfuric acid water surface by Phillips<sup>37</sup> and with infrared spectroscopy measurements of un-ionized molecular hydrates in sulfuric acid.<sup>39</sup> The presence of molecular hydrates has been suggested to play a role in the formation of atmospheric sulfate aerosols,<sup>39</sup> and in the heterogeneous reactivity of sulfuric acid surfaces.<sup>37,38</sup> However, our ability to model  $\alpha$  in terms of the total surface water concentration (eq 12) suggests that the mass accommodation process is unaffected by the formation of molecular hydrates at the surface of sulfuric acid solutions.

## Discussion

Figure 4 compares the behavior of the uptake of several different species on sulfuric acid/water solutions. The values of the mass accommodation ( $\alpha$ ) and uptake ( $\gamma_0$ ) coefficients at 285 K for H<sub>2</sub><sup>17</sup>O(g) and D<sub>2</sub>O(g) on sulfuric acid solutions are shown as a function of H<sub>2</sub>SO<sub>4</sub> concentration (open squares and triangles, respectively). Figure 4 also includes previously published data for the uptake coefficients of H<sub>2</sub><sup>17</sup>O(g) and D<sub>2</sub>O(g) on water<sup>6</sup> and the uptake coefficient of NH<sub>3</sub>(g) on sulfuric acid and water.<sup>40,41</sup>

The measured uptake coefficient for D<sub>2</sub>O is unity, independent of sulfuric acid concentration while the uptake coefficients for H<sub>2</sub><sup>17</sup>O are significantly smaller than unity. Because the mass accommodation coefficients of H<sub>2</sub><sup>17</sup>O and D<sub>2</sub>O are expected to be the same, the enhanced uptake of D<sub>2</sub>O is attributed to the fast isotope exchange reaction D<sub>2</sub>O + H<sub>2</sub>O → 2HDO at the

acidic surface. As a result of this reaction, D<sub>2</sub>O disappears rapidly from the gas phase, yielding a near-unity uptake coefficient. As noted in Li et al.<sup>6</sup> for the case of water and D<sub>2</sub>O uptake on water, the measured value of near unity for the uptake coefficient of D<sub>2</sub>O on sulfuric acid solutions implies that the thermal accommodation coefficient *S* for D<sub>2</sub>O (and therefore H<sub>2</sub>O) is likewise near unity.

As can be seen in Figure 4, the uptake coefficients of H<sub>2</sub>O(g) and NH<sub>3</sub>(g) both increase as a function of increasing H<sub>2</sub>-SO<sub>4</sub> concentration. In the case of ammonia, the plateau at the low acid concentration end is the mass accommodation coefficient of NH<sub>3</sub>(g) on water. The uptake coefficient then rises as acidity increases due to an additional uptake channel provided by surface reaction of ammonia with H<sup>+</sup>: NH<sub>3</sub>(s) + H<sup>+</sup>(s) → NH<sub>4</sub><sup>+</sup>(s). The dash-dot line shows a surface reaction model for NH<sub>3</sub>(g) uptake that is parametrized in terms of the H<sup>+</sup> activity in the solution. In the case of H<sub>2</sub><sup>17</sup>O(g) uptake, the mass accommodation coefficient increases with increasing sulfuric acid concentration due to changes in the relative amounts of water and sulfuric acid at the surface as expressed by eq 12.

**Atmospheric Implications.** The mass accommodation coefficient for water vapor plays a role in determining the size and number distributions of droplets in a forming cloud.<sup>3,4,46,47</sup> As an air parcel rises adiabatically in the troposphere, it cools and its equilibrium water vapor pressure with respect to liquid water decreases. At some point supersaturation reaches a critical value, and water vapor starts to condense on pre-existing particles capable of cloud droplet nucleation. This condensation is the only sink for water vapor in the parcel, and the strength of this sink is determined by the rate of gas-liquid water vapor mass transfer, i.e., either by the rate of water vapor diffusion to the droplet's surface or by the mass accommodation coefficient of water vapor,  $\alpha$ , depending on which process is rate limiting. Slower transfer of water vapor into aerosol particles due to lower values of  $\alpha$  allows higher water vapor supersaturations to build-up. For small values of  $\alpha$  (generally less than 0.1), model calculations indicate that the mass accommodation process is rate limiting and the resulting higher supersaturation levels lead to the activation of a greater fraction of available aerosol particles, producing more, but smaller, cloud droplets than would have occurred with a larger value of  $\alpha$ . This difference in the number and size distribution of droplets can strongly affect both cloud stability against precipitation and cloud light-scattering properties, modifying the influence of clouds on both meteorology and climate.<sup>1,3,48-50</sup>

The measurements presented in this paper of  $\alpha > 0.1$  on sulfuric acid surfaces, combined with previous measurements of  $\alpha > 0.1$  on water surfaces,<sup>6</sup> suggest that  $\alpha$  for water vapor condensation exceeds 0.1 for typical tropospheric cloud formation conditions. This supports cloud physics modeling studies indicating that it is unlikely for  $\alpha$  to be less than 0.1.<sup>47,51,52</sup> Since  $\alpha$  is greater than 0.1, the precise values determined here are not required for simulating the activation of cloud droplets in clean air by normal inorganic aqueous aerosol particles. However, the growth of new sulfuric acid particles with diameters in the 1–50-nm range formed via binary sulfuric acid/water nucleation may be impeded by a kinetic limitation on water vapor uptake. Further, the growth of stratospheric sulfuric acid aerosols, which typically have diameters on the order of 0.1  $\mu\text{m}$ , may also be kinetically constrained by the values of the mass accommodation coefficients presented here.

**Acknowledgment.** This research was supported by the NASA Upper Atmosphere Research Program, contract #NAG2-1462. The authors thank Dr. Lynn Russell for valuable discussions.

## References and Notes

- (1) Climate Change 2001: The Scientific Basis. *Contribution of Working Group I to the Third Assessment Report of the Intergovernmental Panel on Climate Change*; Houghton, J. T., Ding, Y., Griggs, D. J., Noguer, M., van der Linden, P. J., Dai, X., Maskell, K., Johnson, C. A., Eds.; Cambridge University Press: Cambridge, UK, 2001.
- (2) Köhler, H. *Meteorol. Z.* **1921**, *38*, 168.
- (3) Chuang, P. Y.; Charlson, R. J.; Seinfeld, J. H. *Nature* **1997**, *390*, 594.
- (4) Nenes, A.; Ghan, S.; Abdul-Razak, H.; Chuang, P. Y.; Seinfeld, J. H. *Tellus, Ser. B* **2001**, *53*, 133.
- (5) Hallberg, A.; Noone, K. J.; Ogren, J. A. *Tellus, Ser. B* **1998**, *50*, 59.
- (6) Li, Y. Q.; Davidovits, P.; Shi, Q.; Jayne, J. T.; Kolb, C. E.; Worsnop, D. R. *J. Phys. Chem. A* **2001**, *105*, 10627.
- (7) Worsnop, D. R.; Zahniser, M. S.; Kolb, C. E.; Gardner, J. A.; Watson, L. R.; Doren, J. M. V.; Jayne, J. T.; Davidovits, P. *J. Phys. Chem.* **1989**, *93*, 1159.
- (8) Kolb, C. E.; Worsnop, D. R.; Zahniser, M. S.; Davidovits, P.; Keyser, L. F.; Leu, M.-T.; Molina, M. J.; Hanson, D. R.; Ravishankara, A. R.; Williams, L. R.; Tolbert, M. A. Laboratory Studies of Atmospheric Heterogeneous Chemistry. In *Progress and Problems in Atmospheric Chemistry*; Barker, J. R., Ed.; World Scientific Publishing Co.: Singapore, 1995.
- (9) Jayne, J. T.; Worsnop, D. R.; Kolb, C. E.; Swartz, E.; Davidovits, P. *J. Phys. Chem.* **1996**, *100*, 8015.
- (10) Shi, Q.; Li, Y. Q.; Davidovits, P.; Jayne, J. T.; Worsnop, D. R.; Kolb, C. E. *J. Phys. Chem.* **1999**, *103*, 2417.
- (11) Danckwerts, P. V. *Gas-liquid reactions*; McGraw-Hill: New York, 1970.
- (12) Schwartz, S. E. Mass-Transport Considerations Pertinent to Aqueous Phase Reactions of Gases in Liquid-Water Clouds. In *Chemistry of Multiphase Atmospheric Systems*; Jaeschke, W., Ed.; NATO: Brussels, 1986; Vol. G6.
- (13) In our earlier work, the symbol  $\Gamma_{\text{sol}}$  was used to take into account the effects on the uptake of Henry's law solubility. The subscript "sol" caused some confusion since it is also used to designate the solvation rate  $k_{\text{sol}}$ . The solvation process is independent of the uptake limitation due to solubility, and we have therefore changed the subscript of the  $\Gamma$  coefficient from sol to sat.
- (14) Fuchs, N. A.; Sutugin, A. G. *Highly Dispersed Aerosols*; Ann Arbor Science Publishers: Newton, MA, 1970.
- (15) Widmann, J. F.; Davis, E. J. *J. Aerosol Sci.* **1997**, *28*, 87.
- (16) Seinfeld, J. H.; Pandis, S. N. *Atmospheric Chemistry and Physics: From Air Pollution to Climate Change*; John Wiley and Sons: New York, 1998.
- (17) Hanson, D. R.; Ravishankara, A. R.; Lovejoy, E. R. *J. Geophys. Res.* **1996**, *101*, 9063.
- (18) Worsnop, D. R.; Shi, Q.; Jayne, J. T.; Kolb, C. E.; Swartz, E.; Davidovits, P. *J. Aerosol Sci.* **2001**, *32*, 877.
- (19) Morita, A.; Sugiyama, M.; Koda, S. *J. Phys. Chem.* **2003**, *107*, 1749.
- (20) Jayne, J. T.; Duan, S. X.; Davidovits, P.; Worsnop, D. R.; Zahniser, M. S.; Kolb, C. E. *J. Phys. Chem.* **1991**, *95*, 6329.
- (21) Brown, D. E.; George, S. M.; Huang, C.; Wong, E. K. L.; Rider, K. B.; Smith, R. S.; Kay, B. D. *J. Phys. Chem.* **1996**, *100*, 4988.
- (22) Hanson, D. R. *J. Phys. Chem. B* **1997**, *101*, 4998.
- (23) Robinson, G. N.; Worsnop, D. R.; Jayne, J. T.; Kolb, C. E.; Davidovits, P. *J. Geophys. Res.* **1997**, *102*, 3583.
- (24) Zahniser, M. S.; Nelson, D. D.; McManus, J. B.; Keabian, P. L. *Philos. Trans. R. Soc. London, Ser. A* **1995**, *351*, 371.
- (25) Rothman, L. S.; Rinsland, C. O.; Goldman, A.; Massie, S. T.; Edward, D. P.; Flaud, J. M.; Perrin, A.; Camy-Peyret, C.; Dana, V.; Mandin, J. V.; Schroeder, J.; McCann, A.; Gamache, R. R.; Wattson, R. B.; Yoshino, K.; Chance, K. V.; Jucks, K. W.; Brown, L. R.; Nemtchinov, V.; Varansi, P. *J. Quant. Spectrosc. Radiat. Transfer* **1998**, *60*, 665.
- (26) Camy-Peyret, C.; Flaud, J. M.; Mahmoudi, A. *Int. J. Infrared Millimeter Waves* **1985**, *6*, 199.
- (27) Gillen, K. T.; Douglass, D. C.; Hoch, M. J. R. *J. Chem. Phys.* **1972**, *57*, 5117.
- (28) Williams, L. R.; Long, F. S. *J. Phys. Chem.* **1995**, *99*, 3748.
- (29) In a previous paper on the mass accommodation coefficient for water on water, we equated *H* with the gas/liquid partitioning coefficient defined in terms of the liquid concentration of water and the equilibrium vapor pressure,  $H = [\text{H}_2\text{O}(l)]/P_{\text{H}_2\text{O}} = [\text{H}_2\text{O}(l)]/[\text{H}_2\text{O}(g)]RT$ . In that case,

the data showed no time dependence and H estimated as the gas–liquid partitioning coefficient was consistent with no observed time dependence. In the present case, the gas–liquid partitioning coefficient gives  $3.3 \times 10^5$  M atm<sup>-1</sup>, a factor of 6 larger than the value of  $H_{\text{meas}}$  determined from fitting the time dependence of the uptake data.

- (30) Schwertz, F. A.; Brow, J. E. *J. Chem. Phys.* **1951**, *19*, 640.
- (31) Swinton, F. L. Self-diffusion in gaseous CO<sub>2</sub> and H<sub>2</sub>O and the inter-diffusion coefficient of CO<sub>2</sub>/H<sub>2</sub>O mixtures. In *Diffusion Processes*; Sherwood, J., Ed.; Gordon and Breach: London, 1971; Vol. 1.
- (32) Kimpton, D. D.; Wall, F. T. *J. Phys. Chem.* **1952**, *56*, 715.
- (33) Marrero, T. R.; Mason, E. A. *J. Phys. Chem. Ref. Data* **1972**, *1*, 3.
- (34) Davidovits, P.; Hu, J. H.; Worsnop, D. R.; Zahniser, M. S.; Kolb, C. E. *Discuss. Faraday Soc.* **1995**, *100*, 65.
- (35) Kolb, C. E.; Davidovits, P.; Jayne, J. T.; Shi, Q.; Worsnop, D. R. *Prog. React. Kinet. Mech.* **2002**, *27*, 1.
- (36) Li, Y. Q.; Zhang, H. Z.; Davidovits, P.; Jayne, J. T.; Kolb, C. E.; Worsnop, D. R. *J. Phys. Chem. A* **2002**, *106*, 1220.
- (37) Phillips, L. F. *Aust. J. Chem.* **1994**, *47*, 91.
- (38) Shultz, M. J.; Baldelli, S.; Schnitzer, C.; Simonelli, D. *J. Phys. Chem. B* **2002**, *106*, 5313.
- (39) Couling, S. B.; Fletcher, J.; Horn, A. B.; Newnham, D. A.; McPheat, R. A.; Williams, R. G. *Phys. Chem. Chem. Phys.* **2003**, *5*, 4108.
- (40) Swartz, E.; Shi, Q.; Davidovits, P.; Jayne, J. T.; Worsnop, D. R.; Kolb, C. E. *J. Phys. Chem. A* **1999**, *103*, 8824.
- (41) The falloff in NH<sub>3</sub> uptake at lower sulfuric acid concentrations is in good agreement with earlier measurements of Bongartz et al.,<sup>42</sup> Ponche et al.,<sup>43</sup> and Carstens et al.<sup>44</sup> and contradicts more recent measurements of Hanson and Kosciuh.<sup>45</sup> The latter suggest that the uptake coefficient is approximately unity even at their lowest sulfuric acid concentration of 15 wt %.
- (42) Bongartz, A.; Schweighoefer, S.; Roose, C.; Schurath, U. *J. Atmos. Chem.* **1995**, *20*, 35.
- (43) Ponche, J. L.; George, C.; Schurath, U. *J. Atmos. Chem.* **1993**, *16*, 1.
- (44) Carstens, T.; Wunderlich, C.; Schurath, U. *Computational Mechanics*; Southampton, England, 1996.
- (45) Hanson, D. R.; Kosciuh, E. *J. Phys. Chem. A* **2003**, *107*, 2199.
- (46) Hudson, J. G.; Yum, S. S. *J. Atmos. Sci.* **1997**, *54*, 2642.
- (47) Yum, S. S.; Hudson, J. G.; Xie, Y. *J. Geophys. Res.* **1998**, *103*, 16625.
- (48) Charlson, R. J.; Schwartz, S. E.; Hales, J. M.; Cess, R. D.; Coakley, J. A., Jr.; Hansen, J. E.; Hoffman, D. *J. Science* **1992**, *255*, 423.
- (49) Rosenfeld, D. *Science* **2000**, *287*, 1793.
- (50) Fukuta, N.; Walter, L. A. *J. Atmos. Sci.* **1970**, *27*, 1160.
- (51) Leaitch, W. R.; Strapp, J. W.; Isaac, G. A.; Hudson, J. G. *Tellus* **1986**, *388*, 328.
- (52) Hudson, J. G.; Garrett, T. J.; Hobbs, P. V.; Strader, S. R.; Xie, Y. X.; Yum, S. S. *J. Atmos. Sci.* **2000**, *57*, 2696.